[PROC. OF JSCE Structural Eng./Earthquake Eng. Vol. 2, No. 1 April 1985]

AN EXPERIMENTAL STUDY ON SHEARING STRESS CONCENTRATION AT THE CORNER WELD IN TRUSS CHORDS

By Hiromasa TERADA and Tohru NATORI**

Shearing stress concentration at reentrant corner in built-up box section is studied using an electrical analogy. In the built-up box section, for truss chord members, this corner is made usually by partial penetration groove or fillet weld at outside because of the difficulty of welding on inside corner. Therefore, a sharp reentrant corner is induced and high stress concentration may occur. In the case of partial connection, besides, the tortional rigidity is reduced and angular twist increases. The test results show that the stress concentration at weld root of partial penetration is about 2 times higher than that of the rolled section and the tortional rigidity decreases about 35 % in comparison with that of fully penetrated section.

1. INTRODUCTION

In stiffening truss members for long span suspension bridges, box sections composed by fillet weld or/and partial penetration weld are generally used. Assuming that truss members undergo only normal force, corner weld may not be so significant in stresses.

For all practical purposes, shearing force, twisting moment and bending moment added to normal force apply to truss members by various actions, resulting in corner welds being under composite stresses. In the case of suspension bridges for roadways and railways, fatigue strength and strss concentration of these corner welds becomes a subject of discussion under composite stresses[1].

Stress concentration in the reentrant corner of a round or square tube in torsion has been analyzed and calculated many times, but owing to its greater mathematical difficulty, those of tubes of other sections to say nothing of the corner with fillet or partial penetration weld are not treated[2].

At the roots of partial weld and fillet weld, there may be sharp notches and it is easily supposed that a considerable stress concentration may take place at these corners. Furthermore the existence of unwelded parts in the corner may influence on the tortional rigidity of the box section[3].

From these points of view, experimental studies were practised for the welded corner details.

The membrane analogy by soap film is very useful in enabling us to visualize the stress distribution over the cross section. But at point of the stress concentration, as at fillets of small radius, the soap film method is likely to yield inaccurate results. So, an electrical analogy has been used. This mehod is based on the general equation for the flow of an electric current in a thin homogeneous plate being identical with that of tortional problems of hollow sections. Accuracy to within a few percent may be obtained and moreover this method is more economical than the finite element method by the help of computer[4),4)].

* Member of JSCE, Yokogawa Bridge Works (88 Shinminato, Chiba-shi, Chiba)

2. THEORETICAL BACKGROUND

An interesting case is the solution of Poissons' equation with constant boundary conditions. An example is the St. Venant problem of bars of hollow sections.

The equation is :

$$\frac{\partial^2\phi}{\partial x^2}+\frac{\partial^2\phi}{\partial y^2}=-2G\theta \quad \cdots\cdots (1)$$

G : shear modulus of elasticity

θ : angle of twist per unit length

ϕ : stress function

By the following transformation

$$\phi=\psi-\frac{1}{2}(x^2+y^2)G\theta$$

Eq. (1) is reduced to Laplace equation (2)

$$\frac{\partial^2\psi}{\partial x^2}+\frac{\partial^2\psi}{\partial y^2}=0 \quad \cdots\cdots (2)$$

For simply connected regions, $\phi=0$ on the boundary. This problem may be solved by the electric analog method if a constant current (uniformly distributed over the surface of the model) is applied to the surface and the boundary of the model is held at a constant potential by means of some device to fit the boundary.

The voltage distribution then obeys the equation :

$$\frac{\partial^2 V}{\partial X^2}+\frac{\partial^2 V}{\partial Y^2}=0 \quad \cdots\cdots (3)$$

From Eq. (2) and (3), one need only set up a voltage distribution on the boundary that corresponds to the condition $\phi=0$, that is, $\psi=(x^2+y^2)G\theta/2$ and measure the voltage distribution over the surface of the model corresponding to ϕ.

$$\phi=KV-\frac{1}{2}(x^2+y^2)G\theta \quad \cdots\cdots (4)$$

where $K=\psi/V$, which is called analogous coefficient.

The shear stresses and torque then are

$$\tau_{xz}=\frac{\partial\phi}{\partial y}, \quad \tau_{yz}=-\frac{\partial\phi}{\partial x}, \quad T=2\int_F \phi dF$$

3. EXPERIMENTAL APPARATUS, PROCEDURE AND TEST MODEL

Fig. 1 shows the assumed cross section of a truss chord member and one of the models which is cut out at the corner and enlarged 3 times as long as it, for the sake of accurate measurement.

The conducting material is agar of 2 % density and the concentration of NaCl in it is 1 %.

The vessel for agar is made of acrylic resin plates and its depth is 9 mm constant.

Fig. 2 shows a schematic drawing of the power supply consisting of a large number of voltage dividers all fed from a common voltage source. In practice, the required boundary voltage specified by $\psi=(x^2+y^2)G\theta/2$ varies continuously. This is difficult to achieve practically, but this condition can be approximated by applying the voltage in discrete steps along the boundary. The voltage dividers were set at 10 mm spaces for the corner and at 20 mm spaces for the ordinary boundary. Electrodes were 6 mm wide copper plates.

An a-c voltage was applied between the outer boundary and inner boundary, through the a-c current stabilizing equipment of output power 20 V, constant frequency 400 Hz (NF CIRCUIT DESIGN BROCK, POWER AMPLIFIER MODEL TA-250).

Voltage measurements were made with an electron voltmeter that could be easily read to 1/100 of a volt.

Photo 1 shows a typical layout of model with connections, the power supply and the voltmeter.

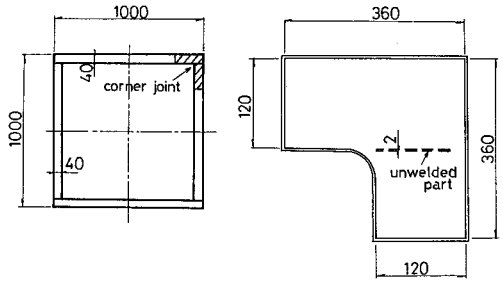

Assumed cross section　　Experimental model (enlaraged by 3 times)

Fig. 1 Assumed cross section and one of the experimental models.

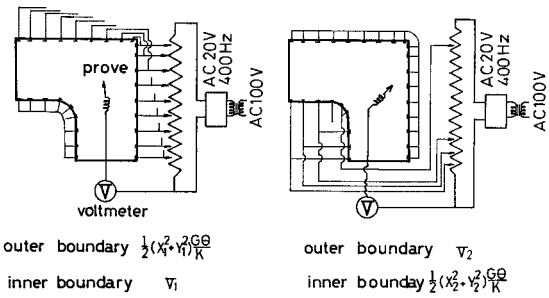

Fig. 2 Schematic drawing of the power supply.

Table 1 The relation between ϕ and V (the hollow section).

	Ager surface	Outer boundary	Inner boundary
ϕ	$\phi=\phi_a+\phi_b$	$\phi_o=\phi_1+\frac{1}{2}(x_1^2+y_1^2)G\theta$	$\phi_1=\phi_2+\frac{1}{2}(x_2^2+y_2^2)G\theta$
	ϕ_a	$\frac{1}{2}(x_1^2+y_1^2)G\theta$	ϕ_2
	ϕ_b	ϕ_1	$\frac{1}{2}(x_2^2+y_2^2)G\theta$
V	$V=V_a+V_b$	$V_o=V_1+\frac{1}{2}(X_1^2+Y_1^2)\frac{G\theta}{K}$	$V_1=V_2+\frac{1}{2}(X_2^2+Y_2^2)\frac{G\theta}{K}$
	V_a	$\frac{1}{2}(X_1^2+Y_1^2)\frac{G\theta}{K}$	V_2
	V_b	V_1	$\frac{1}{2}(X_2^2+Y_2^2)\frac{G\theta}{K}$

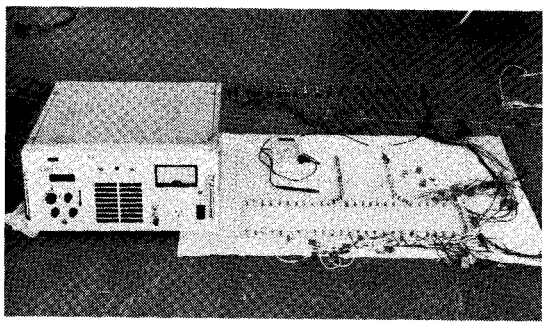

Photo 1 Experimental apparatus.

When the section contains one or more holes, two or more measurements are needed to know the values of the torsional function ϕ on the boundaries. The analogical relation betwwen ϕ and V and boundary conditions are shown in Table 1, for example, to hollow section with one hole.

At first, the various divided voltages specified by $V_o=(X_1^2+Y_1^2)\,G\theta/2\,K$ are set along outer boundary under the connecting condition of equal voltage at inner boundary. Voltages V_2 at inner boundary and V_a at agar surface are then mesured by a probe and voltmeter.

At second procedure, the inner electrodes are set to required boundary condition voltage $V_i=(X_2^2+Y_2^2)\,G\theta/2\,K$ and the outer electrodes are all connected to be equal potential. And again, the voltage measurements are made for V_1 at outer boundary and for V_b at agar surface.

The desired voltages are then read for each prove position and the final answer is the sum of all the individual voltage readings.

4. TEST PROGRAM

The series of corner details tested are as follows;

Fundamental series : full penetration welding joints

Series A : joints composed of fillet weld by inside as well as partial penetration weld by outside

Series B : joints composed of both side welds, in which the thickness of flange plate and web plate is not same

Series C : fillet welding joints by outside

Fundamental series consists of two specimens of perfectly connected corner, aiming at the confirmation of test fitness and at obtaining the basic data to compare with the results of other series. One is the model of practical cross section shown in Fig. 1 and the other is for the cross section composed of thicker plates compared with the first one.

Series A is of practically used details and consists of five specimens, in which the sizes of fillet and partial penetration welds are varied respectively.

In series B, the thicknesses of flange and web plates are changed to know how the direction and length of the non-welded portion in corner influence on shearing stress distribution and stress concentration.

Series C consists of two specimens of fillet welding joints by outside, which are used for smaller box sections of truss bridge members in general.

Table 2 shows the specimens of each series, in which the dimensions are converted into practical section by one-third of the test models.

5. TEST RESULTS

(1) Test results on the thin-walled section and the thick-walled section

Fig. 3 shows the lines of shearing stress, and the torsional stress function ϕ as well as the shearing stress distribution in the direction of plate thickness at the corner and the ordinary part. Shearing stress lines shown here represent the contour lines of the torsional stress function.

Table 2 The specimen of test series.

Series	Type of weld	Configuration	Case No.	Dimension (mm)
Fundamental Series	full penetration weld	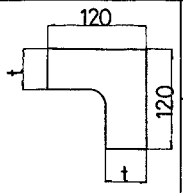	F1	1000x1000 t =40 r =12
			F2	240x 240 t =60 r =20
A Series	V-groove weld	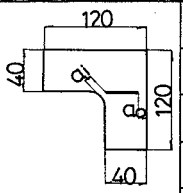	A1	ao = 9 ai = 0
	V-groove and fillet weld		A2	ao = 9 ai = 5
			A3	ao = 9 ai = 9
			A4	ao = 7 ai = 7
			A5	ao = 5 ai = 9
B Series	V-groove and fillet weld	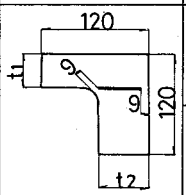	B1	t1 = 40 t2 = 60
			B2	t1 = 60 t2 = 40
C Series	fillet weld	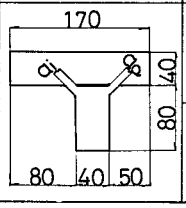	C1	ao = 9.4 ai = 0
	fillet weld on bothside		C2	ao = 9.4 ai = 8.5

In the case of the thin-walled section F1, the shearing stress line distributs uniformly in the direction of plate thickness at the ordinary part and its spacing changes gradually closer to the inner boundary, which means the stress concentration. Test values and calculated values obtained on the assumption that the plate thickness is fully thin cpmpared with the sectional dimension, are shown in Table 3. In this calculation, it

Table 3 Comparison of experimental value with calculated value for Case A1.

		Experimental Value	Calculated Value
Torsional Moment T		$3.72\times10^{10}G\theta$	$(3.72\times10^{10}G\theta)$
Angle of twist θ		θ	1.05θ
Shearing stress	Ordinary part	$503G\theta$	$504G\theta$
	Corner weld	$1198G\theta$	$1084G\theta$
	Concentration factor (α)	2.38	2.15

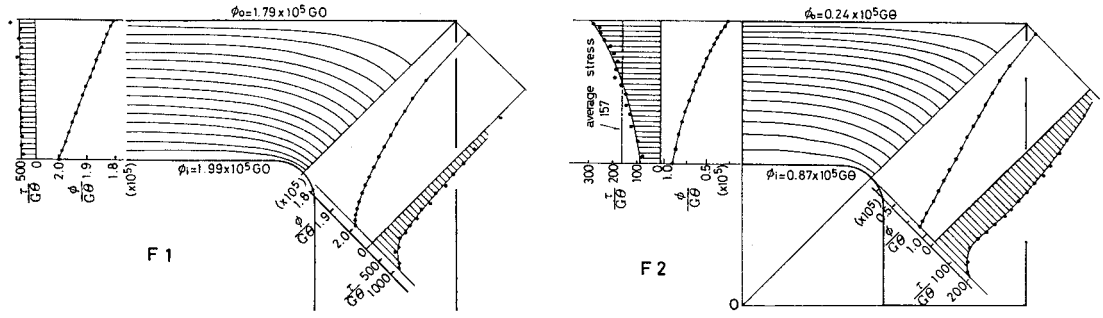

Fig. 3 Test results of Fundamental series.

is assumed that regions adjacent to external corners of the joint do not have any relation to the sharing of stresses and the corner has constant thickness. Besides, applied torsional moment T in calculation is provided the same as that obtained from test results.

From Table 3, it is clear that the shearing stresses at the ordinary part and the angle of twist θ are nearly equal in both experimental and theoretical results. Therefore, if the ratio of the cross sectinal dimension to the plate thickness is in the same degree as this model, it may be concluded that the thin-walled theory used heretofore is effective. The ratio of shearing stress at the reentrant corner versus that at the ordinary part, that is the factor of the stress concentration α, is $\alpha=2.38$ in the experiment against $\alpha=2.15$ in the calculation. The difference between the experimental and the calculated value may be mostly caused by the assumption given above.

In the case of the thick-walled section F2, in which the plate thickness is extremely large compared with the cross sectional dimension, the shearing stress at the ordinary part is not constant, indicating the parabolic distribution that the maximum stress is at the outer boundary and minimum stress is at the inner boundary. This distributed configuration is similar to that of the solid section. Consequently, it is obvious that the application of the thin-walled theory is limited for this case.

(2) Joints composed of the fillet weld by inside as well as the partial penetration weld by outside (A Series)

Fig. 4 shows the test results on the corner joint A1 composed by the V-groove weld of the outside corner only and the joint A2 composed by the V-groove weld and the inside fillet weld. The standard weld size of V-groove weld on the outside corner was taken at 9 mm which was derived from size $S=\sqrt{2t}$, and the size of the fillet weld, $S=7$ mm (throat thickness of about 5 mm).

The shearing stress line of A1 takes a roundabout way to the welded zone of the outside corner, showing the considerable stress concentration at the tip of the non-deposited zone (root of weld). The shearing stress at the root of the weld is $\tau=5485\,G\theta$ and when compared with the average stress at the throat section, the factor of the stress concentration becomes $\alpha=3.7$. In addition, the thickness is reduced from 40 mm at the ordinary part to 9 mm at the weld throat, resulting in the increment of the shearing stress of $40/9=4.4$. The stress at the weld root, therefore, becomes 16 times ($=4.4\times3.7$) as larger as the shearing stress at the ordinary part.

When the corner is composed by the outer weld and the inner weld, shearing stress lines are divided into both the outside and inside weld. Blank areas of the shearing stress at the base metal across the non-deposit zone do not contribute to the stress transfer together with the regions of external angles at the

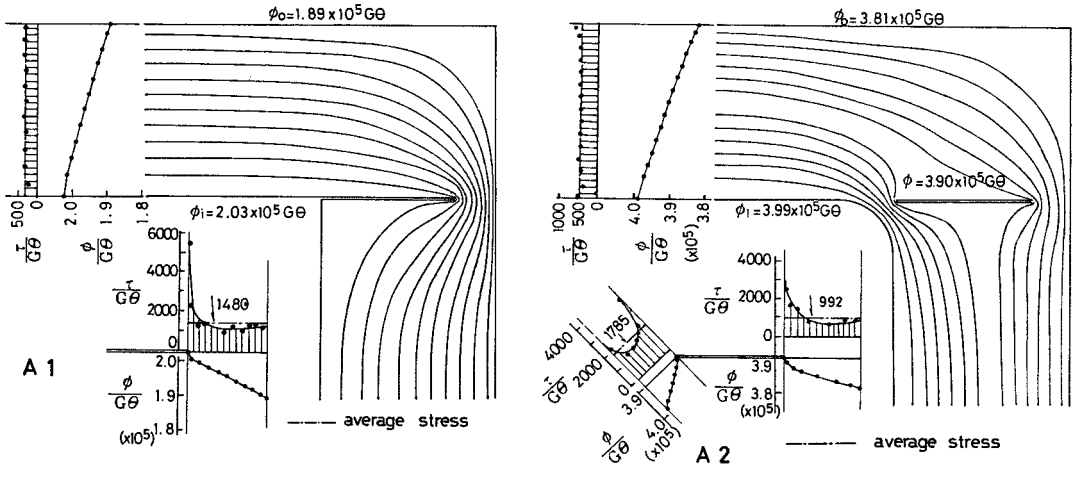

Table 4 Test results of A Series.

		A 2 a_o=9 a_i=5	A 3 a_o=9 a_i=9	A 4 a_o=7 a_i=7	A 5 a_o=5 a_i=9
Shear flow	q	17850	19167	19763	19380
	q_o	8925(0.50)	7778(0.41)	8288(0.42)	7523(0.39)
	q_i	8925(0.50)	11389(0.59)	11475(0.58)	11857(0.61)
Average shearing stress	$\tau=q/t$	446	479	494	485
	$\tau_o=q_o/a_o$	992	864	1184	1505
	τ_o/τ	2.2	1.8	2.4	3.1
	$\tau_i=q_i/a_i$	1785	1267	1639	1317
	τ_i/τ	4.0	2.6	3.3	2.7
Shearing stress at the root	$\tau_{o,r}$	2998	3070	4264	5160
	α_o	3.0	3.6	3.6	3.4
	$\tau_{i,r}$	3632	2800	3618	2816
	α_i	2.0	2.2	2.2	2.1
Maximum concentration factor	α'_o	6.6	6.5	8.6	10.5
	α'_i	8.0	5.7	7.3	5.7

$(q,\tau)\times G\theta$; ( ): q_o/q, q_i/q ; t=40mm

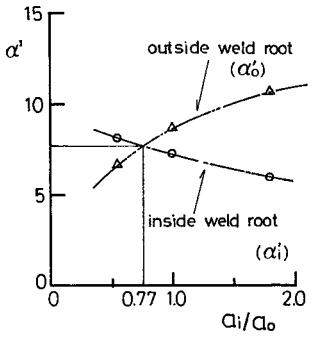

Fig. 5 The relation between a_i/a_o and α'.

corner. In the case of A2, the stress concentration is $\alpha=3.0$ at the root of the outside weld and $\alpha=2.0$ at the root of the inside weld. Accordingly, the co-use of the inside weld moderates to some extent the stress concentration on the outside weld root, but it is noted that it also produces another point of the stress concentration.

Table 4 shows the test results of Series A in which weld sizes are varied. In Table 4, q represents the shear-flow at the ordinary part and q_o, q_i represent the shear-flow to the outside and inside weld zones respectively. Shear-flow q is described generally as $q=\tau t$ in the the thin-walled hollow section. Here, because of the uneven distribution of the shearing stress at corner welds, q_o and q_i are calculated by the equation $q_{o,i}=\int_0^{a_{o,i}} \tau da$. τ represents the average shearing stress at the ordinary part. τ_o, τ_i are the average shearing stress of the weld throat and τ_{or}, τ_{ir} are the shearing stress at the roots of the outside and inside weld respectively. α'_o, α'_i are the ratio of the stress at the root of each weld to that of the ordinary part.

Case A2, A4 and A5 in Table 4 have the same total throat thickness of the outside and inside weld. The relation of the throat thickness ratio of a_i/a_o and α'_i, α'_o in these cases is ploteed in Fig. 5.

When the throat thickness of the outside and inside weld are equal, a large amount of the shear-flow runs through in the inside weld and consequently the ratio of the shear-flow of the inside weld to the outside weld becomes about 6 : 4. In ordr to equalize the average shearing stress of the outside and inside weld, the throat thickness of the inside weld is 1.6 times larger than that of the outside weld based on $q_o/a_o=q_i/a_i$. When it is necessary to consider the maximum shearing stress as in the case of the fatigue strength, it is desirable to make $a_i/a_o=0.77$, taking the condition of $\alpha'_o=\alpha'_i$ as can be seen in Fig. 5. So, assuming total throat thickness to be 14 mm, the throat thickness of the inside weld may be taken at 6 mm and that of the outside weld 8 mm.

Next, the torsional resistance will be discussed. Torsional moment T that is otained from the stress function ϕ is shown as follow.

Case F1 : $T_{F1}=3.72\times10^{10}\, G\theta_{F1}$

Case A1 : $T_{A1}=2.47\times10^{10}\, G\theta_{A1}$, $a_i=0$ mm

Case A2 : $T_{A2}=3.33\times10^{10}\, G\theta_{A2}$, $a_i=5$ mm

Case A3 : $T_{A3}=3.54\times10^{10}\, G\theta_{A3}$, $a_i=9$ mm

Case A4 : $T_{A4}=3.66\times10^{10}\, G\theta_{A4}$, $a_i=7$ mm

Case A5 : $T_{A5}=3.59\times10^{10}\, G\theta_{A5}$, $a_i=9$ mm

If the angle of twist θ is taken as $\theta_{F1}=\theta_{Ai}$ $(i=1\sim5)$, the torsional moment as compared with the completely penetrated weld joint F1 is 0.66 times in the joint A1 with the outside weld only, 0.90 times in

the joint A2 with the outside weld and the inside weld of a_i=5 mm and more than 0.95 times in the joints A 3, A4 and A5 of $a_i \geqq 7$ mm. In other words, when the corner of the box section is jointed by imperfect welds the torsional resistance of the box section falls below the rigidity supposed in design and results in the occurence of larger torsional deformation than that in design proccedure. This tendency is especially significant in the box section composed of the partial penetration weld at the outside only. Lowering of the torsional resistance is improved by adding the inside weld, but even in this case, it is preferable that the throat thickness of the inside weld is over 5 mm.

As mentioned above, the torsional rigidity is reduced by the exsistence of the non-deposited portion. In the following, it will be shown how to take into consideration the plate thickness to get the corresponding to the rigidity of the box section jointed by partial penetration welds at the corner, taking case A1 for example.

The torsional resistance of the hollow section is

$$J=\frac{4F^2}{\oint \frac{ds}{t}}+C\sum bt^3 \fallingdotseq \frac{4F^2}{\oint \frac{ds}{t}} \quad \cdots\cdots (6)$$

For convenience it is assumed that area F, where F is the mean of the area enclosed by the outer and inner boundary of the cross section, does not change even if there are non-welded parts and the effects of web plates with the non-welded part only are taken into consideration. When the web thickness is represented by t_{we}, the torsional resistance of Case A1 is

$$J_{A1}=\frac{4\times 96^4}{2\left(\frac{96}{4}+\frac{96}{t_{we}}\right)}=0.66\,J_{F1}=0.66\frac{4\times 96^4}{4\times\frac{96}{4}} \quad \cdots\cdots (7)$$

$\therefore\ t_{we}=2$ cm

Accordingly, when the box section is composed by the partial penetration V-groove outside weld of a generalized throat thickness ($S=\sqrt{2}\,t$), the torsional resistance will be equivalent to the value of the cross section calculated as 1/2 of the web thickness is effective.

(3) Joints composed of difference thickness plates (B Series)

When the thicknesses of the flange and web plates of the box section differ from each other, the length of the non-deposited portion depends on which plate is thicker. Furthermore, since the distribution width of the shear-flow differs in the flange and web plate, it is considered that the ratio of the shear-flow on the outside and inside weld is different from that of the case with equal thicknesses.

Test results of two cassses B1, B2, where in B1 the flange plate is thicker than the web plate and in B 2 that relation is reversed, are shown in Table 5 together with Case A3 having equal plate thickness. In this series, the joints were composed of both side welds, and each throat thickness of the ouside and inside weld was taken at 9 mm.

When the angle of twist is assumed to be constant, the torsional moment of B1 and B2 increase as compared with A3. This is because the torsional resistance is improved by the increment of the plate thickness. The increment of the torsional resistance of Case B1 is 16 percent and of case B2, 22 percent compared with A3 in test and that is 17 percent in calculation. It could be considered therfore that the length of the non-deposited portion (B1 : 51 mm, B2 : 31 mm) have influence on the torsional rigidity.

The shear-flow reduces in the outside weld and

Table 5 Test results of B Series.

(x GΘ)

			With difference plate thickness		With equal plate thickness
			B 1	B 2	A 3
Torsional Moment T			4.12×10^{10}	4.33×10^{10}	3.54×10^{10}
Shear-flow	q		22 695	23 843	19 167
	q_o		8 925 (0.39)	11 093 (0.47)	7 778 (0.41)
	q_i		13 770 (0.61)	12 750 (0.53)	11 389 (0.59)
Stress	Ordinary part	t=40	567	596	480
		t=60	378	397	—
	at the root	outside τ_o	992	1 233	864
		inside τ_i	1 530	1 417	1 265

( ): q_o/q , q_i/q

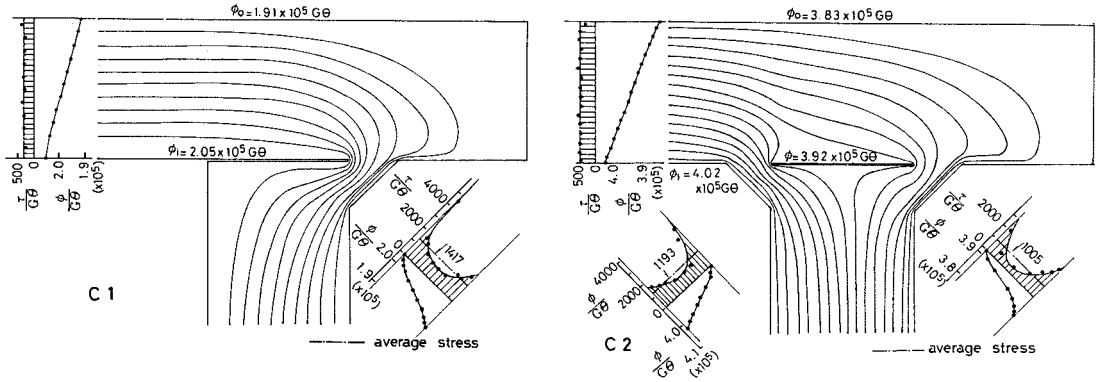

Fig. 6 Test results of C Series.

concentrates in the inside weld, when the non-deposited portion is longer (B1). On the contrary, when the flange is thicker and non-deposited portion is relatively short (B2), the ratio of the shear-flow in the outside weld increases. Consequently, the maximum shearing stress coefficient becomes $\alpha'=7.2$ under the stress concentration of the root $\alpha=3.6$. It is noted therfore that the length of the non-deposited portion will differ according to the way of increase the plate thickness, and the distribution characteristics of the shearing stress and maximum shearing stress will be considerably influenced, even if the formation of the box section is similar.

(4) Fillet welding joints by outside (C Series)

The test results on the corners with the protrudent leg, in which one is composed of the outside fillet weld (C1) and the other is composed of both side fillet welds (C2), are shown in Fig. 6. In these corners, the bead surface of the fillet weld was taken as a straight line because the stress concentration at the bead surface was not critical as seen in test results shown heretofore. And the throat thicknesses in terms of a real structure were $a_o=9.4$ mm and $a_i=8.5$ mm.

The paths of the shearing stress line tend to shift more to the outer side in the case of outside fillet weld only (C1) than in the case with the V-groove welding A1, and a higher stress concentration of $\alpha=4.0$ occures in the root of the fillet weld. When compared with the Case A1, α of the fillet weld exceeds that of the groove weld by 10 percent.

Torsional moment $T=2.47\times10^{10}\ G\theta$ of C1 is equivalent to that of the V-groove weld A1. Therefore, it is obvious that the protrudent legs do not contribute to the rise of torsional rigidity.

When the inside fillet weld is used together with the outside weld (C2), a shear-flow runs more into the inside weld and as a result the stress concentration at the outside fillet weld is moderated to $\alpha=3.0$. However, the stress concentration is $\alpha=2.9$ at the root of the inside weld which is virtually the same as that developed in the root of the outside weld. Furthermore, the stress concentration at the bead surface becnmes $\alpha=2.4$. Therefore, it is observed that points of stress concentration are enlarged when the fillet welding is used.

6. SUMMARY

The characteristics of the shearing stress distribution, the extent of the stress concentration and the maximum coefficient of the shearing stress were clarified using an electrical analogy for such of the welded corner of the box section as that of large truss members under torsion. The experimental results are as follows.

(1) The results obtained from experiments carried out on the box section (assumed dimension of 1 000 $\times$1 000$\times$40 mm) indicated that the values of the shearing stress at the ordinary part were virtualy constant. Therefore, the thin-walled theory which has been used heretofore can be fully applied when the

ratio of the cross sectional dimension to plate thickness is about the same as that given above.

(2) In the case of a hollow cross section with the plate thickness being extremely large compared to the cross sectional dimension (240×240×60 mm), the parabolic distribution of the shearing stress is gained in the plate thickness direction similar to that of a solid cross section. Therefore, it is clear that there is a limit in application of the thin-walled theory and the electrical analogy used here is useful for the analysis of these thick-walled hollow sections, too.

(3) In the case of the box section formed with the partial V-groove weld on the outside of the corner and taking the throat thickness at $\sqrt{2}\,t$, the shearing stress concentration at the root of the weld against the average shearing stress of the throat section becomes $\alpha=3.7$. When the reduction of the cross section of the corner weld zone is taken into consideration, the shearing stress of the root is 16 times the ordinary part. This value is considerably large and it may be required to check the fatigue safety when the truss chord member accepts repeated torsional moment.

(4) Moreover, the torsional resistance of the structural member with partial welded corner lowers to 66 % compared to the corner section that is perfectly jointed. In order to accurately evaluate the torsional resistance or deformation, it is necessary to carry out the calculation as about 1/2 of the web thickness having the non-deposited portion is efficient.

(5) When the outside and inside of the corner are welded simultaneously, the torsional resistance can be held to about 10 percent lower. But in this case, it is desirable to make the throat thickness of the inside weld greater than 5 mm . The shear-flow to the weld on the outside and inside is not proportional to each throat thickness, and the rate of burden of the flow to the inside weld rises. Hence, it is necessary to make large the size of the weld on the inside in order to equaleze the average shearing stress in the outside and inside welds.

(6) When the fatigue strength becomes a problem, the maximum shearing stress of corner weld zones must be taken into consideration. Above all, the stress concentration at the root of welds on the outside and inside, and the ratio of burden of the shear-flow must be considered to equalize the maximum shearing stress. In other words, it is preferable to hold the throat size ratio between the inside and outside weld to be $a_i/a_o=0.77$.

(7) When the box section is formed with different thickness plates, it is necessary to exercise care since the shear-flow changes and the maximum shearing stress is influenced by the length of the non-deposited portion.

(8) In the case of the fillet welding on the outside with protrudent legs provided on the flange, the stress concentration is higher at $\alpha=4.0$ as compared to the V-groove weld, even if the throat thickness is about the same as that of the V-groove weld. The fillet weld used on the inside together changes the shear-flow, and it moderates to some extent the stress concentration at the root of the outside fillet weld. But there is also a generation of stress concentrations of about $\alpha=3.0$ and 2.4 at the root of the inside weld and bead surface, respectively.

REFERENCES

1) Sasado, S., Yoshikawa, N., Kawai, A. and Mizumoto, Y. : Design and Construction of Corner Joint on Large Span Truss Bridge. Journal of The Bridge and Foundation Engineering. No. 3, 1975.
2) Timoshenko and Goodier : Theory of Elasticity, Second Edition, pp. 288~299.
3) Nakazawa, H. : On the Torsion of a Shaft by Means of the Electrolytic Tank Analogy, Trans. of JSME, Vol. 22, No. 119, pp. 484~488.
4) Nakazawa, H. : Electrical Analogies with Resistive Paper for the Torsion Bar, Trans. of JSME, Vol. 23, No. 127, pp. 194~197.
5) Swannell, J. H. : The Torsion Problem-A New Twist, Experimental Mechanics, pp. 279~284.

(Received May 17 1984)